Reductively Degradable α-Amino Acid-Based Poly(ester amide)-Graft-Galactose Copolymers: Facile Synthesis, Self-Assembly, and Hepatoma-Targeting Doxorubicin Delivery

Journal:	*Biomaterials Science*
Manuscript ID:	BM-ART-12-2014-000436.R2
Article Type:	Paper
Date Submitted by the Author:	18-Mar-2015

Complete List of Authors:	Lv, Jiaolong; Soochow University, College of Chemistry, Chemical Engineering and Materials Science Sun, Huanli; Soochow University, College of Chemistry, Chemical Engineering and Materials Science Zou, Yan; Soochow University, College of Chemistry, Chemical Engineering and Materials Science Meng, Fenghua; Soochow University, College of Chemistry, Chemical Engineering and Materials Science Dias, Aylvin; DSM, Biomedical Hendriks, Marc; DSM, Biomedical Feijen, Jan; University of Twente, Polymer chemistry and biomaterials Zhong, Zhiyuan; Soochow University, College of Chemistry, Chemical Engineering and Materials Science

SCHOLARONE™
Manuscripts

Reductively Degradable α-Amino Acid-Based Poly(ester amide)-*Graft*-Galactose Copolymers: Facile Synthesis, Self-Assembly, and Hepatoma-Targeting Doxorubicin Delivery

Jiaolong Lv[1], Huanli Sun[1], Yan Zou[1], Fenghua Meng[1,*], Aylvin A. Dias[2], Marc Hendriks[2], Jan Feijen[1,3], and Zhiyuan Zhong[1,*]

[1] Biomedical Polymers Laboratory, and Jiangsu Key Laboratory of Advanced Functional Polymer Design and Application, College of Chemistry, Chemical Engineering and Materials Science, Soochow University, Suzhou, 215123, P. R. China.

[2] DSM Biomedical, Koestraat 1, Geleen 6167 RA, The Netherlands.

[3] Department of Polymer Chemistry and Biomaterials, Institute for Biomedical Technology and Technical Medicine (MIRA), Faculty of Science and Technology, University of Twente, Enschede, The Netherlands.

* Corresponding authors. Tel/Fax: +86-512-65880098, Email: fhmeng@suda.edu.cn (F. Meng); zyzhong@suda.edu.cn (Z. Zhong)

Novel reductively degradable α-amino acid-based poly(ester amide)-graft-galactose (SSPEA-Gal) copolymers were designed and developed to form smart nano-vehicles for active hepatoma-targeting doxorubicin (DOX) delivery. SSPEA-Gal copolymers were readily synthesized via solution polycondensation reaction of di-*p*-toluenesulfonic acid salts of bis-L-phenylalanine 2,2-thiodiethanol diester and bis-vinyl sulfone functionalized cysteine hexanediol diester with dinitrophenyl ester of adipic acid, followed by conjugating with thiol-functionalized galactose (Gal-SH) via the Michael addition reaction. SSPEA-Gal formed

unimodal nanoparticles (PDI = 0.10-0.12) in water, in which average particle sizes decreased from 138 to 91 nm with increasing Gal contents from 31.6 wt.% to 42.5 wt.%. Notably, *in vitro* drug release studies showed that over 80% DOX was released from SSPEA-Gal nanoparticles within 12 h under an intracellular mimicking reductive environment, while low DOX release (< 20%) was observed for reduction-insensitive PEA-Gal nanoparticles under otherwise the same condition and SSPEA-Gal nanoparticles under a non-reductive condition. Notably, SSPEA-Gal nanoparticles exhibited high specificity to asialoglycoprotein receptor (ASGP-R)-overexpressing HepG2 cells. MTT assays using HepG2 cells showed that DOX-loaded SSPEA-Gal had a low half maximal inhibitory concentration (IC_{50}) of 1.37 μg/mL, approaching that of free DOX. Flow cytometry and confocal laser scanning microscopy studies confirmed the efficient uptake of DOX-loaded SSPEA-Gal nanoparticles by HepG2 cells as well as fast intracellular DOX release. Importantly, SSPEA-Gal and PEA-Gal nanoparticles were non-cytotoxic to HepG2 and MCF-7 cells up to a tested concentration of 1.0 mg/mL. These tumor-targeting and reduction-responsive degradable nanoparticles have appeared as an interesting multi-functional platform for advanced drug delivery.

Keywords: α-amino acid; poly(ester amide); biodegradable nanoparticles; reduction-sensitive; targeted drug delivery; hepatocellular carcinoma.

Introduction

Biodegradable polymers such as polyesters, polycarbonates, and polypeptides are key biomaterials that play a pivotal role in biomedical technology.[1-6] In recent years, poly(ester amide)s (PEAs), in particular α-amino acid-based PEAs, have emerged as a novel class of biodegradable polymers that show a tremendous potential in various biomedical applications

including implant coatings, gene delivery and tissue engineering.[7-14] In contrast to aliphatic polyesters such as poly(lactic acid) (PLA), poly(ε-caprolactone) (PCL), and poly(glycolic acid) (PGA), PEAs are highly functional and versatile in which polymers with vastly different structures and functionalities along the main chains and/or at the side chains, have been reported.[15-19] Unlike other types of functional biodegradable polymers, α-amino acid-based PEAs are conveniently prepared by solution polycondensation reaction. It should further be noted that α-amino acid-based PEAs are subject to hydrolytic as well as enzymatic degradation (e.g. by α-chymotrypsin).[18,20-23] α-Amino acid-based PEAs have elegantly combined unique features of polypeptides and polyesters. Notably, in spite of their obvious advantages, there are no reports on development of stimuli-responsive drug delivery systems from α-amino acid-based PEAs.

In the past several years, reduction-sensitive degradable nanoparticles have received particular attention for enhanced intracellular drug and protein delivery,[24-28] taking advantage of the fact that there is a high reducing potential inside the tumor cells, which is about 2-3 orders of magnitude higher than that in the extracellular environment including blood.[29,30] The work from different groups has demonstrated that reduction-responsive polymeric nanocarriers exhibit significantly improved *in vitro* and *in vivo* antitumor efficacy as compared to their reduction-insensitive counterparts.[31-34] The synthesis of reduction-responsive biocompatible and biodegradable polymeric systems, nevertheless, is not straightforward and often involves multiple steps. It should also be noted that to enhance their tumor specificity, cellular uptake and therapeutic efficacy, reduction-responsive biodegradable nanoparticles are additionally obliged to be equipped with specific targeting ligands.[35-39]

In this paper, we report on smart nano-vehicles based on novel reduction-sensitive degradable α-amino acid-based poly(ester amide)-graft-galactose (SSPEA-Gal) copolymers

for active hepatoma-targeting doxorubicin (DOX) delivery (Scheme 1). β-D-galactose (Gal) is a specific targeting ligand to asialoglycoprotein receptor (ASGP-R) on mammalian hepatocytes, which provides a useful means for targeted chemotherapy of liver cancers.[40,41] Notably, galactosamine-PHPMA-GFLG-DOX (PK2), the first active tumor-targeting polymeric nanomedicine, has been translated to the human clinical trials.[42] The clinical results showed that liver-specific DOX delivery is achievable using PK2 and targeting is witnessed in primary hepatocellular tumors. Inspired by these clinical results, we have recently designed and explored galactose-decorated degradable nanocarriers for hepatoma-targeting anticancer drug delivery *in vitro*[38,39] as well as *in vivo*[43,44]. In order to construct hepatoma-targeting and reductively degradable nanoparticles, functional PEAs (SSPEA) containing multiple disulfide linkages on their main chains and vinyl sulfone at their side chains were designed and synthesized from solution polycondensation reaction of di-*p*-toluenesulfonic acid salts of bis-L-phenylalanine 2,2-thiodiethanol diester and bis-vinyl sulfone functionalized cysteine hexanediol diester with dinitrophenyl ester of adipic acid. SSPEA-Gal could be readily obtained by post-polymerization modification SSPEA with thiol-functionalized galactose via the Michael addition reaction. Here, the synthesis of SSPEA-Gal copolymers, nanoparticle preparation and DOX loading, reduction triggered drug release, hepatoma-targetability and *in vitro* anti-tumor activity of DOX-loaded micellar nanoparticles were investigated.

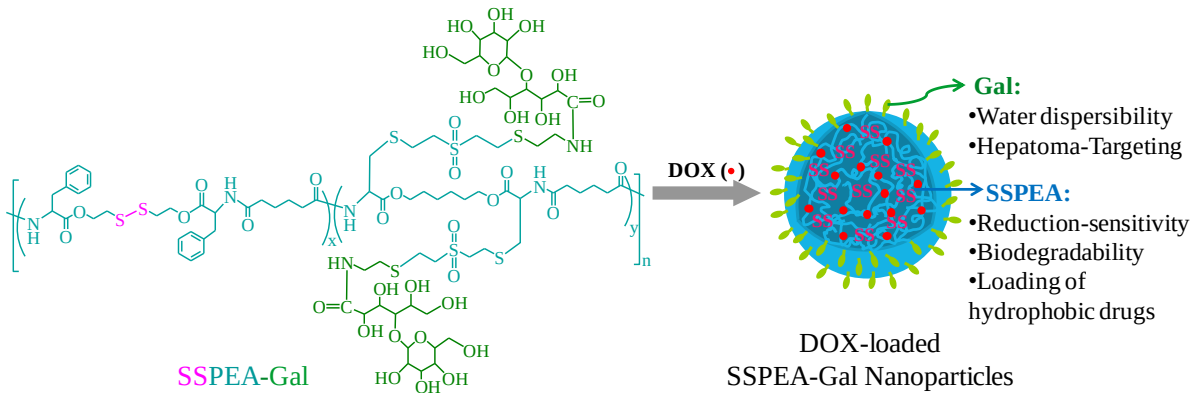

Scheme 1 Illustration of hepatoma-targeting reductively degradable nanoparticles based on SSPEA-Gal copolymers.

Experimental section

Materials

2,2-Thiodiethanol (TDE, 98%, ABCR), triethylamine (Et_3N, 99%, Alfa Aesar), 1,4-dithio-$_{DL}$-threitol (DTT, 99%, Merck), lactobionic acid (LBA, 97%, Acros), L-phenylalanine (Phe, 99%, Aladdin), 1,6-hexanediol (97%, Alfa Aesar), L-cysteine hydrochloride monohydrate (cysteine, 99%, Alfa Aesar), divinyl sulfone (95%, Dalian Guanghui Chemical Co., Ltd, China), 2-mercaptoethylamine hydrochloride (99%, Alfa Aesar), glutathione (reduced form, GSH, 99%, Roche), *p*-toluenesulfonic acid monohydrate ($TsOH·H_2O$, 97.5%, J&K), and doxorubicin hydrochloride (DOX·HCl, > 99%, Beijing ZhongShuo Pharmaceutical Technology Development Co., Ltd.) were purchased and used as-received. Toluene were dried by refluxing over sodium wire and distilled prior to use. N,N-dimethyl ormamide (DMF) and dimethyl sulfoxide (DMSO) were dried by refluxing over CaH_2 and distilled before use. Thiol-containing galactose (Gal-SH) and dinitrophenyl ester of adipic acid (Di-NP-AA) were synthesized according to previous reports.[39,45] Other reagents were analytical grade and used without further purification.

Characterizations

^{1}H NMR spectra were recorded on a Unity Inova 400 spectrometer operating at 400 MHz using D_2O or DMSO-d_6 as solvents. The chemical shifts were calibrated against solvent signals. The molecular weight and polydispersity of the copolymers were determined by a Waters 1515 gel permeation chromatograph (GPC) instrument equipped with two linear PLgel columns (500 Å and Mixed-C) following a guard column and a differential refractive-index detector. The measurements were performed using DMF as the eluent at a flow rate of 1.0 mL/min at 30 ºC and a series of narrow polystyrene standards for the calibration of the columns. Fourier transform infrared spectrometer (Varian 3600 FTIR) was

performed on Thermo Scientific spectrophotometer with Omnic software for data acquisition and analysis. Samples were grounded into KBr powder and pressed into discs prior to FTIR analysis. The hydrodynamic sizes and size distribution of nanoparticles were determined using dynamic light scattering (DLS) at 25 ºC by a Zetasizer Nano-ZS from Malvern Instruments equipped with a 633 nm He/Ne laser using back-scattering detection. Transmission electron microscopy (TEM) was performed using a Tecnai G220 TEM operated at an accelerating voltage of 200 kV. The samples were prepared by dropping 10 μL of 0.1 mg/mL nanoparticles suspension on the copper grid followed by staining with 1 wt.% phosphotungstic acid.

Synthesis of di-p-toluenesulfonic acid salt of L-phenylalanine 2,2-thiodiethanol diester (Phe(TDE)·2TsOH)

Phe(TDE)·2TsOH was synthesized via the reaction of L-phenylalanine (L-Phe) with 2,2-thiodiethanol (TDE) in the presence of *p*-toluenesulfonic acid monohydrate ($TsOH \cdot H_2O$). Briefly, under a nitrogen atmosphere, L-Phe (6.00 g, 36.3 mmol), HES (2.546 g, 16.5 mmol) and $TsOH \cdot H_2O$ (6.909 g, 36.3 mol) in 92 mL of toluene (20 mL for Dean-Stark) were placed in a flask equipped with a magnetic stirrer, a Dean-Stark apparatus and a $CaCl_2$ drying tube. The solid-liquid reaction mixture was heated to reflux for 8 h until 1.25 mL of water was evolved and the reaction mixture changed to ivory-white. 7 mL of ethanol was added after the reaction mixture was cooled to below 60 ºC. The mixture was further cooled to room temperature (r.t.), filtered, washed twice using a mixture of toluene and ethanol (10/1 v/v) and dried in vacuo at r.t.. The product was purified by re-crystallization from methanol/water (1/1 v/v) three times. The final product Phe(TDE)·2TsOH was obtained as white crystals. Yield: 78.7%. ^{1}H NMR (DMSO-d_6): δ 2.29 (6H, $\underline{CH_3}$-Ph-SO_3-), 2.86 (4H, -$\underline{CH_2}$-S-S-), 3.11 (4H, Ph-$\underline{CH_2}$-), 4.33 (6H, 4H of -COO-$\underline{CH_2}$-CH_2-S-S- and 2H of ^+H_3N-$\underline{CH}$(CH_2PH)-COO-), 8.41

(6H, $^{+}\underline{H_3N}$-CH(CH_2PH)-), 7.10-7.49 (18H, Ph). ^{13}C NMR (100 MHz, DMSO-d_6): δ 168.9 (-$\underline{C}OO$-$\underline{CH_2}$-CH_2-S-S-), 145.3, 137.8, 134.5, 127.3 (CH_3-$\underline{Ph}$-SO_3-), 129.4, 128.4, 128.1, 125.4 ($\underline{Ph}$-CH_2-), 63.1 (-COO-$\underline{CH_2}$-CH_2-S-S-), 53.2 ($^{+}H_3N$-$\underline{CH}$(CH_2PH)-COO-), 36.0 (-COO-CH_2-$\underline{CH_2}$-S-S-), 35.5 ($^{+}H_3N$-CH($\underline{CH_2}$PH)-), 20.8 ($\underline{CH_3}$-Ph-SO_3-). Element analysis for Phe(TDE)·2TsOH ($C_{36}H_{44}N_2O_{10}S_4$): C: 56.67%; H: 6.18%; N: 4.42%. Found: C: 56.85%; H: 5.94%; N: 4.53%. FTIR (Stretching vibration peaks) (cm^{-1}): 3000 (-NH_3^{+}), 1735 (-CO-), 1450, 1500 and 1600 (-Ph), 1202 (-SO_3^{-}).

The synthesis of di-p-toluenesulfonic acid salt of L-phenylalanine hexanediol ester (Phe(HD)·2TsOH) was conducted similarly just replacing TDE with 1,6-hexanediol. Yield: 81.4%.

Synthesis of di-*p*-toluenesulfonic acid salt of vinylsulfone substituted cysteine ester (VSC(HD)·2TsOH)

Under a nitrogen atmosphere, to a methanol solution (200 mL) of divinyl sulfone (29.40 g, 249 mmol), a solution of cysteine hydrochloride monohydrate (3.364 g, 19.0 mmol) in 50 mL of methanol was added dropwise at 30 ºC. After completion of addition, the reaction was allowed to proceed for 60 h in the dark. The resulting vinylsulfone substituted cysteine (VC) was isolated by concentration, precipitation in cold ethyl acetate and drying in vacuo. Yield: 69.4%. ^{1}H NMR (400 MHz, D_2O): δ 6.36~6.95 (3H, vinyl), 4.22 (1H, NH_3^{+}-$\underline{CH}$(-CH_2)-COO-), 3.57 (2H,-CH_2-(O=)S=O-), 3.19 (2H, -CH–$\underline{CH_2}$-S-) and 2.97 (2H, -S-$\underline{CH_2}$-CH_2-).

To synthesize VSC(HD)·2TsOH, VC (1.00 g, 3.6 mmol), 1,6-hexanediol (0.195 g, 1.6 mmol), TsOH·H_2O (0.908 g, 4.8 mmol) and 2-methoxyhydroquinone (10 mg) in 20 mL of toluene were placed in a flask equipped with a magnetic stirrer, a Dean-Stark apparatus and a $CaCl_2$ drying tube. The solid-liquid reaction mixture was heated to reflux for 8 h and the

reaction mixture was brown oily. The reaction mixture was cooled to r.t. and the product was isolated by dissolving in methanol, precipitation in cold ether three times and drying in vacuo at r.t.. Yield: 85.8%. ^{1}H NMR (400 MHz, D_2O): δ 4.44 (2H, NH_3^+-*CH*(-CH_2)-COO-), 3.55 (4H, -*CH*$_2$-SO_2-), 3.25 (4H, -S-*CH*$_2$-CH_2-), 2.96 (4H, -CH-*CH*$_2$-S-), 6.36~6.95 (6H, vinyl), 4.30 (4H, -COO-*CH*$_2$-), 1.73 (4H, -COO-CH_2-*CH*$_2$-), 1.43 (4H, -COO-CH_2-CH_2-*CH*$_2$-), 7.36, 7.70 (8H, Ph) and 2.40 (6H, *CH*$_3$-Ph-SO_3-). ^{13}C NMR (100 MHz, DMSO-d_6): δ 168.1 (-*COO*-CH_2-CH_2-CH_2-), 145.2, 137.9, 136.5, 130.5 (CH_3-*Ph*-SO_3-), 128.1 (*CH*$_2$(CH)$SO_2CH_2CH_2$S-), 125.1 (*CH*$_2$(*CH*)$SO_2CH_2CH_2$S-), 66.0 (-COO-*CH*$_2$-CH_2-CH_2-), 52.8 ($^{+}H_3$N-*CH*CH_2-), 51.8 (*CH*$_2$(CH)SO_2*CH*$_2$$CH_2$S-), 31.5 (-COO-$CH_2$-*CH*$_2$-$CH_2$-), 27.8 (*CH*$_2(CH)SO_2CH_2$*CH*$_2$S-), 24.8 ($^{+}H_3$N-CH*CH*$_2$-), 24.3 (-COO-$CH_2$-$CH_2$-*CH*$_2$-), 24.0 (*CH*$_3$-Ph-$SO_3$-). Element analysis for VSC(HD)·2TsOH ($C_{34}H_{52}N_2O_{14}S_6$): C: 44.18%; H: 6.18%; N: 3.82%. Found: C: 44.35%; H: 6.09%; N: 3.62%.

Synthesis of SSPEA and reduction-insensitive PEA

SSPEA was synthesized via solution polycondensation reaction of Phe(TDE)·2TsOH and VSC(HD)·2TsOH with dinitrophenyl ester of adipic acid (Di-NP-AA) [45]. Briefly, under a nitrogen atmosphere, to a Schlenk bottle equipped with a magnetic stir bar were charged Phe(TDE)·2TsOH (0.2596 g, 0.3274 mmol), VSC(HD)·2TsOH (0.2965 g, 0.3274 mmol), Di-NP-AA (0.2567 g, 0.6614mmol), Et_3N (0.203 mL, 1.455 mmol) and 0.35 mL of DMF. After 20 min degassing with nitrogen flow, the reaction vessel was sealed and immersed in an oil bath thermostated at 70 ºC. The reaction was allowed to proceed for 48 h. The resulting polymer was isolated by dilution with DMF, precipitation in ethyl acetate two times to remove nitrophenol, precipitation in water to remove Et_3N·TsOH and drying in vacuo at r.t.. Yield: 32.4%. ^{1}H NMR (400 MHz, DMSO-d_6): δ 4.45 (-NH-*CH*(-CH_2)-COO-, -HN-*CH*(CH_2Ph)-COO-), 3.55 (-*CH*$_2$-SO_2-), 3.05 (-S-*CH*$_2$-CH_2-), 2.96 (-CH-*CH*$_2$-S-), 6.36

(-CH_2-SO_2-*CH*=CH_2), 6.95 (-CH_2-SO_2-*CH*=*CH_2*), 4.10 (-COO-*CH_2*-), 2.03 (-COO-CH_2-*CH_2*-), 1.43 (-COO-CH_2-CH_2-*CH_2*-), 2.86 (-*CH_2*-S-S-), 3.01 (Ph-*CH_2*-), 4.14 (-COO-*CH_2*-CH_2-S-S-), 8.24 (-*HN*-CH(CH_2Ph)-), 7.10-7.4 (*Ph*), 7.44 (-Ph-NO_2). M_n (^{1}H NMR) = 5900 g/mol. M_n (GPC) = 7700 g/mol, PDI (GPC) = 1.46.

The synthesis of PEA and ^{1}H NMR analysis were the same as for SSPEA copolymers except that Phe(TDE)·2TsOH was replaced with Phe(HD)·2TsOH. Yield: 48.4%. M_n (^{1}H NMR) = 6800 g/mol. M_n (GPC) = 8300 g/mol, PDI (GPC) = 1.53.

Synthesis of SSPEA-Gal and PEA-Gal (reduction-insensitive control)

Under a nitrogen atmosphere, to a Schlenk flask equipped with a magnetic stir bar were charged SSPEA (118 mg, 0.210 mmol of vinyl sulfone group), Gal-SH (219 mg, 0.525 mmol)[39], and DMSO (3 mL). After 20 min degassing with nitrogen flow, the reaction vessel was sealed and immersed in an oil bath thermostated at 30 ºC. The reaction was allowed to proceed for 24 h. The crude product was purified by dialysis (MWCO 1000) against deionized water at r.t. for 48 h and lyophilization. Yield: 64.7%. ^{1}H NMR (400 MHz, DMSO-d_6): δ 8.24 (-*HN*-CH(CH_2Ph)-), 7.10-7.4 (Ph), 4.8-5.4 (Gal), 4.45 (-NH-*CH*(-CH_2)-COO-, -HN-*CH*(CH_2Ph)-COO-), 4.14 (-COO-*CH_2*-CH_2-S-S-), 4.10 (-COO-*CH_2*-), 3.55 (-*CH_2*-SO_2-), 3.05 (-S-*CH_2*-CH_2-), 3.01 (Ph-*CH_2*-), 2.96 (-CH-*CH_2*-S-), 2.86 (-*CH_2*-S-S-), 2.03 (-COO-CH_2-*CH_2*-), 1.43 (-COO-CH_2-CH_2-*CH_2*-).

PEA-Gal was synthesized in a similar way except using PEA to replace SSPEA. Yield: 70.6%.

Micelle formation and critical aggregation concentration (CAC) determination

SSPEA-Gal and PEA-Gal micellar nanoparticles were prepared by dropwise addition of 0.8 mL water to 0.2 mL of copolymer solution (0.1 wt.%) in DMSO under constant stirring at r.t.

followed by extensive dialysis (Spectra/Pore, MWCO 7000) against deionized water with 5 times change of dialysis medium. The size was determined by DLS and CAC by fluorometry using pyrene as a fluorescence probe [38,39,44].

The colloidal stability of SSPEA-Gal nanoparticles in PBS (pH 7.4, 10 mM, 150 mM NaCl) containing 10% serum was monitored by DLS at 37 °C in terms of the changes in size and size distribution.

Reduction-triggered destabilization of SSPEA-Gal nanoparticles

Briefly, to 1.5 mL SSPEA-Gal nanoparticles in PBS at 37 °C was added GSH (final GSH concentration is 10 mM). The solution was shaken at 200 rpm at 37 °C. At different time intervals, the changes of size and size distribution of nanoparticles were determined by DLS. SSPEA-Gal nanoparticle dispersions in the absence of GSH and PEA-Gal nanoparticle dispersions in the presence of 10 mM GSH were used as controls.

Encapsulation and reduction-triggered release of DOX

In this study, desalted DOX was used as a model hydrophobic anticancer drug. DOX was obtained by desalting DOX·HCl using triethylamine in DMSO. DOX-loaded nanoparticles were prepared by dropwise addition of 0.8 mL deionized water to a solution of SSPEA-Gal or PEA-Gal copolymers in DMSO (2 mg/mL, 0.2 mL) containing 80 μg DOX (theoretical DOX loading content is 16.7 wt.%) under stirring, followed by dialysis (MWCO of 3500) against deionized water at r.t. for 10 h with 5 times change of the dialysis media. To determine drug loading content (DLC) and drug loading efficiency (DLE), 100 μL of DOX-loaded nanoparticles were freeze-dried, dissolved in 3 mL of DMSO and analyzed with fluorescence spectroscopy (FLS920, ex. 480 nm), wherein the calibration curve was obtained with DOX solutions with different concentrations in DMSO. DLC and DLE were determined according

to the following formula:

DLC (*wt*. %) = (weight of loaded drug/total weight of loaded drug and polymer) ×100

DLE (%) = (weight of loaded drug/weight of drug in feed) ×100.

The *in vitro* release profiles of DOX from SSPEA-Gal nanoparticles were studied at 37 °C in PBS (10 mM, pH 7.4) with 10 mM GSH or PBS only, respectively. 0.5 mL of the above nanoparticles was transferred to dialysis tubes (MWCO 12000–14000), which were immersed into 20 mL of corresponding buffer. The release media was stirred at 37 °C. At desired time intervals, 5 mL release media was taken out and replenished with an equal volume of fresh media. The amount of DOX released was determined by using fluorescence measurement (FLS920, ex. 480 nm). The release experiments were conducted in triplicate and the results presented are the average data with standard deviations.

MTT assays

The antitumor activity of DOX-loaded hepatoma-targeting SSPEA-Gal nanoparticles in ASGP-R over-expressing human hepatoblastoma cell line (HepG2) was studied by MTT assays. MCF-7 cells (low ASGP-R expression) were used as a negative control. In brief, HepG2 or MCF-7 cells were seeded into a 96-well plate (1.0×10^4 cells/well) under 5% CO_2 atmosphere at 37 °C in 90 μL of DMEM containing 10% FBS, 1% L-glutamine, antibiotics penicillin (100 IU/mL) and streptomycin (100 mg/mL) for 24 h. The medium was replaced by 90 μL of fresh DMEM medium, and 10 μL of DOX-loaded SSPEA-Gal nanoparticle dispersion, DOX-loaded PEA-Gal nanoparticle dispersion, or free DOX solution (DOX concentrations from 1.0×10^{-3} to 20 μg/mL) was added. The cells were cultured in DMEM medium at 37 °C under 5% CO_2 atmosphere for another 48 h. 10 μL of 3-(4,5-dimethylthiazol-2-yl)-2,5-diphenyltetrazoliumbromide (MTT) solution (5 mg/mL in PBS) was added and incubated for 4 h at 37 °C. The media were aspirated, and 150 μL of

DMSO was added to dissolve the MTT-formazan generated by live cells. The optical density was measured using a microplate reader (Multiskan FC, Thermo Scientific). The relative cell viability (%) was determined by comparing the absorbance at 570 nm with control wells containing only cell culture medium. Data are presented as average ± SD (n = 4). The statistical significance was evaluated using Student's *t* test.

To evaluate the specificity of DOX-loaded SSPEA-Gal nanoparticles to HepG2 cells, 10 μL of DOX-loaded nanoparticle dispersion or free DOX solution was added into HepG2 or MCF-7 cells in 96-well plates (1×10^4 cells per well) and incubated for 4 h. The medium was replaced by 100 μL of fresh DMEM medium and the cells were cultured for another 44 h. After that, the cell viability was determined in a similar way as described above.

For competitive inhibition experiments, HepG2 and MCF-7 cells were pretreated with lactobionic acid (LBA, 2 mg/mL) for 4 h to block the ASGP-R receptors on the cell surface before adding DOX-loaded SSPEA-Gal nanoparticles.

The cytotoxicity of SSPEA-Gal42 and PEA-Gal42 micellar nanoparticles to HepG2 and MCF-7 cells was determined in a similar way at varying nanoparticle concentrations of 0.2, 0.4, 0.6, 0.8 and 1.0 mg/mL.

Cellular uptake and intracellular DOX release studied by CLSM

MCF-7 or HepG2 cells were cultured on microscope coverslips in a 24-well plate (5×10^4 cells/well) under 5% CO_2 atmosphere at 37 °C using DMEM medium containing 10% FBS, 1% L-glutamine, antibiotics penicillin (100 IU/mL) and streptomycin (100 mg/mL). After 24 h, the medium was replaced by 450 μL of fresh DMEM and 50 μL of prescribed amounts of DOX-loaded SSPEA-Gal nanoparticles, DOX-loaded PEA-Gal nanoparticles or free DOX (dosage: 10 μg DOX equiv./mL). The cells were incubated for 4 h at 37 °C in a humidified 5% CO_2-containing atmosphere. The culture medium was removed and the cells on the

coverslips were rinsed three times with PBS. The cells were fixed with 4% paraformaldehyde and the cell nuclei were stained with DAPI. The fluorescence images of cells were obtained with confocal laser scanning microscope (Leica, TCS SP5).

Flow cytometry studies

HepG2 cells were seeded onto 6-well plates (1×10^6 cells/well) for 24 h using 2 mL DMEM medium containing 10% FBS, 1% L-glutamine, antibiotics penicillin (100 IU/mL) and streptomycin (100 mg/mL). After 24 h incubation, the medium was replaced by 1.8 mL of fresh DMEM and 0.2 mL of DOX-loaded SSPEA-Gal nanoparticles, DOX-loaded PEA-Gal nanoparticles or free DOX (dosage: 10 μg DOX equiv./mL). After 4 h incubation at 37 ºC, the cells were digested by 0.25 w/v% trypsin/0.03 w/v% EDTA. The suspensions were centrifuged at 2000 rpm for 8 min, pelleted in eppendorf tubes, washed twice with cold PBS, and then resuspended in 500 μL of PBS. Fluorescence histograms were recorded with a BD FACSCalibur (Beckton Dickinson, USA) flow cytometer and analyzed using Cell Quest software. 10,000 gated events were analyzed to generate each histogram and the gate was arbitrarily set for the detection of DOX fluorescence.

For competitive inhibition experiments, HepG2 cells were pretreated with LBA (2 mg/mL) for 4 h before adding DOX-loaded SSPEA-Gal nanoparticles to block the ASGP-R receptors on the cell surface. The media were aspirated and replaced by fresh cell culture media. After that, the same procedure was carried out as described above.

Results and Discussion

Synthesis of SSPEA-Gal Copolymers

SSPEA-Gal copolymers were synthesized in two steps: (i) solution polycondensation reaction of di-*p*-toluenesulfonic acid salts of bis-L-phenylalanine 2,2-thiodiethanol diester

(Phe(TDE)·2TsOH) and bis-vinyl sulfone functionalized cysteine hexanediol diester (VSC(HD)·2TsOH) with dinitrophenyl ester of adipic acid (Di-NP-AA), providing the VS-functionalized SSPEAs; and (ii) treatment of VS-functionalized SSPEAs with thiolated galactose (Gal-SH) (Scheme 2). Phe(TDE)·2TsOH was readily obtained by esterification reaction between L-Phe and TDE in the presence of *p*-toluenesulfonic acid (Scheme S1). ^{1}H NMR showed characteristic signals of TDE (δ 2.86 and 4.21) and L-Phe (δ 3.11, 4.33, 7.10-7.49 and 8.42) moieties (Fig. S1A). The signals at δ 3.8 assignable to the methylene protons of TDE next to the hydroxyl group completely disappeared and new resonance emerged at δ 4.21, indicating quantitative esterification. The signals at δ 3.11, 2.86, 2.29 had an integral ratio close to theoretical value (2:2:3). ^{13}C NMR and element analysis results further confirmed the successful synthesis of Phe(TDE)·2TsOH (Fig S1B).

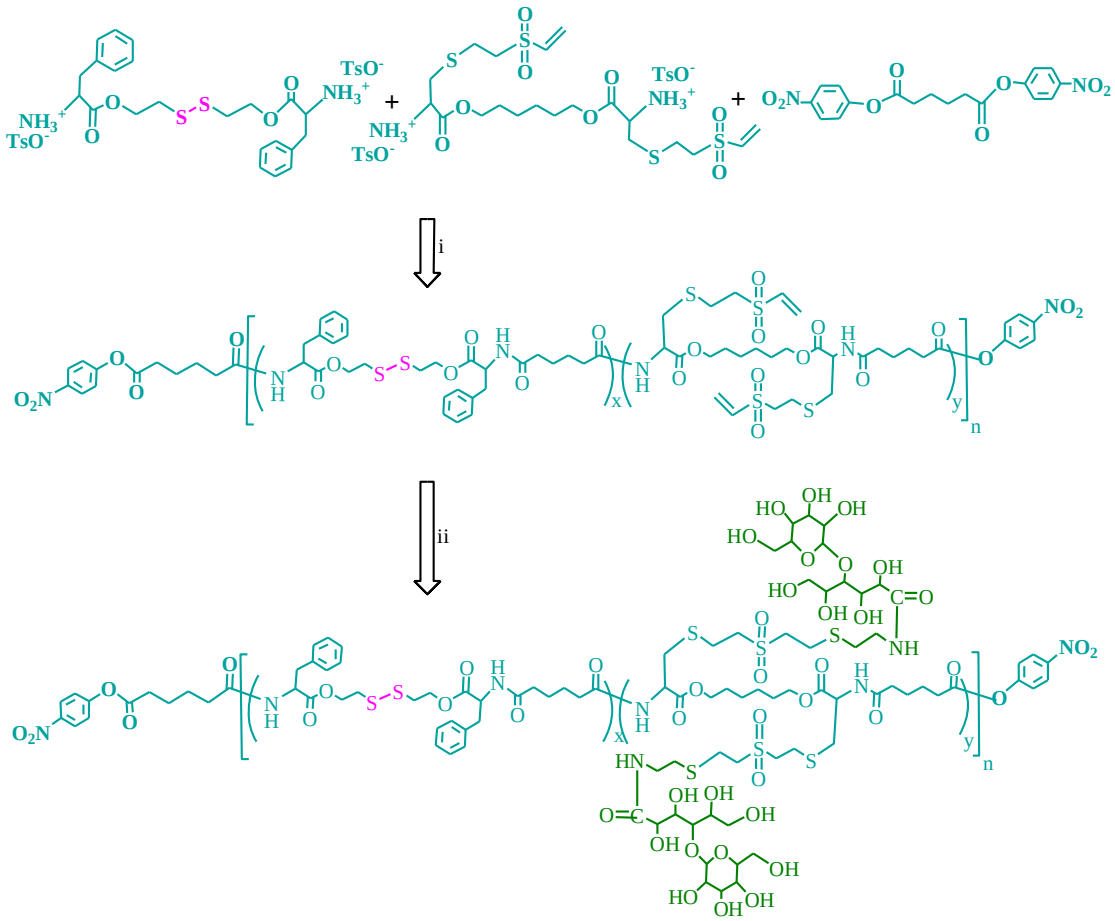

Scheme 2 Synthesis of SSPEA-Gal copolymers. Conditions: (i) Et_3N, DMF, 70°C, 2 d; (ii) Gal-SH, DMSO, r.t., 24 h.

VSC(HD)·2TsOH was prepared by treating cysteine hydrochloride with divinyl sulfone to yield vinyl sulfone substituted cysteine (VSC), followed by esterification with 1,6-hexanediol (Scheme S2). The structure of VSC has been confirmed by ^{1}H NMR (Fig. S2) and FTIR (Fig. S4). ^{1}H NMR of VSC(HD)·2TsOH showed characteristic peaks of VSC moieties at δ 2.97, 3.57 and 6.3~6.95, 1,6-hexanediol moieties at δ 1.43 and 1.73, and TsOH at δ 7.36 and 7.70 (Fig. S3A). The integral ratio of peaks at of δ 1.73, 3.25, and 4.44 was close to the theoretical value of 2:2:1. ^{13}C NMR and element analysis results corroborated the successful synthesis of VSC(HD)·2TsOH (Fig S3B).

The solution polycondensation reaction was carried out in DMF at 70°C at a fixed [Di-NP-AA]/[Phe(TDE)·2TsOH+VSC(HD)·2TsOH] molar ratio of 1.01/1 and [Phe(TDE)·2TsOH]/[VSC(HD)·2TsOH] molar ratios of 7/3 or 5/5 (Table 1). ^{1}H NMR of the resulting SSPEA polymer displayed resonances assignable to Di-NP-AA moieties (δ 2.00 and 1.43), Phe(TDE) moieties (δ 2.86, 3.01, 4.24, 4.45, 7.20 and 8.24) and VSC(HD) moieties (δ 1.33, 1.73, 2.96, 3.25, 3.55, 4.3, 4.45, 6.36~6.95), respectively (Fig. 1A). The molar ratio of [Phe(TDE)]/[VSC(HD)] in the copolymers could be determined by comparing the integrals of signals at δ 4.45 and 6.36. The DP and number-average molecular weight (M_n) were determined from ^{1}H NMR end group analysis by comparing the integrals of signals at δ 6.36 and 7.45 (p-nitrophenol end groups). The results showed that thus-obtained copolymers had compositions close to the design (Table 1). The M_n decreased from 6.9 to 5.9 kg/mol with decreasing [Phe(TDE)·2TsOH]/[VSC(HD)·2TsOH] molar ratios from 7/3 to 5/5. The M_n determined by GPC, though showed some deviation likely due to use of polystyrene as standards, was in parallel with those from ^{1}H NMR end group analysis. These SSPEA copolymers had moderate polydispersity indexes of 1.43 to 1.46.

Table 1 Characteristics of SSPEA and PEA with different compositions

Entry	Polymer	[Phe(TDE)]/[VSC(HD)] or [Phe(HD)]/[VSC(HD)] ratio		M_n (g/mol)		M_w/M_n[d]
		Design[a]	Determined[b]	^{1}H NMR[c]	GPC[d]	
1	SSPEA	7/3	6.9/3.1	6900	9200	1.43
2		5/5	4.6/5.4	5900	7700	1.46
3	PEA	5/5	4.8/5.2	6800	8300	1.53

[a] Molar ratio of Phe(TDE) or Phe(HD) to VSC(HD) in feed;

[b] Molar ratio of Phe(TDE) or Phe(HD) to VSC(HD) determined by ^{1}H NMR;

[c] Determined by ^{1}H NMR end group analysis. M_n was calculated according to the following formulus: $M_n = M_1 \times X + M_2 \times Y + M_3$, wherein X and Y representing numbers of Phe(TDE) containing repeating unit (repeating unit 1) and VSC(HD) containing repeating unit (repeating unit 2) were obtained by comparing the integrals of signals at δ 4.45 and 6.36, respectively, to that at δ 7.45 (p-nitrophenol end groups). M_1, M_2 and M_3 representing the molecular weights of repeating units 1 and 2, and Di-NP-AA are equal to 558, 670 and 388 g/mol, respectively.

[d] Determined by GPC (eluent: DMF, flow rate: 0.5 mL/min, standards: polystyrene).

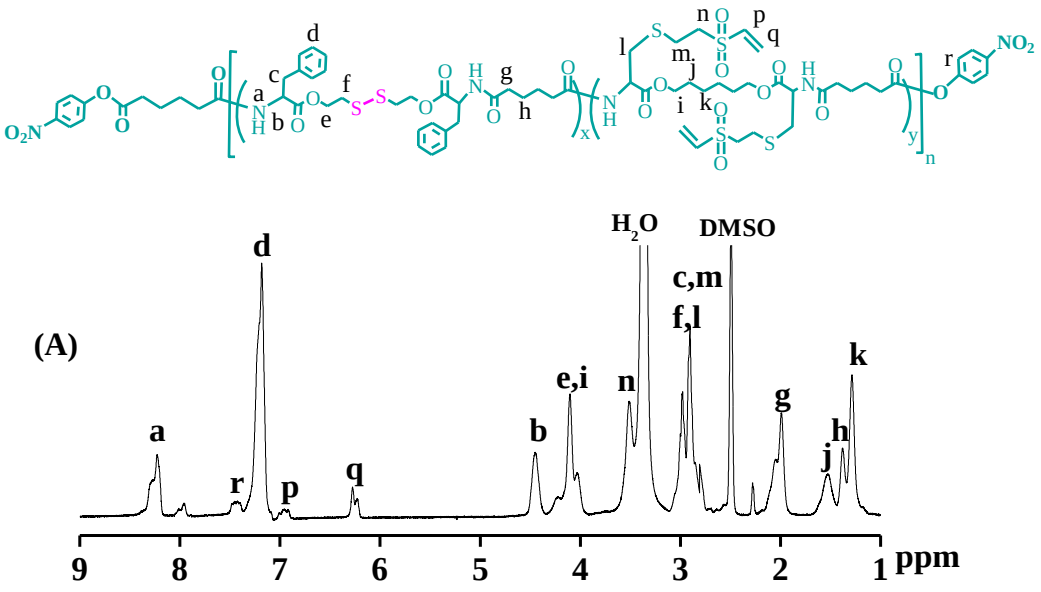

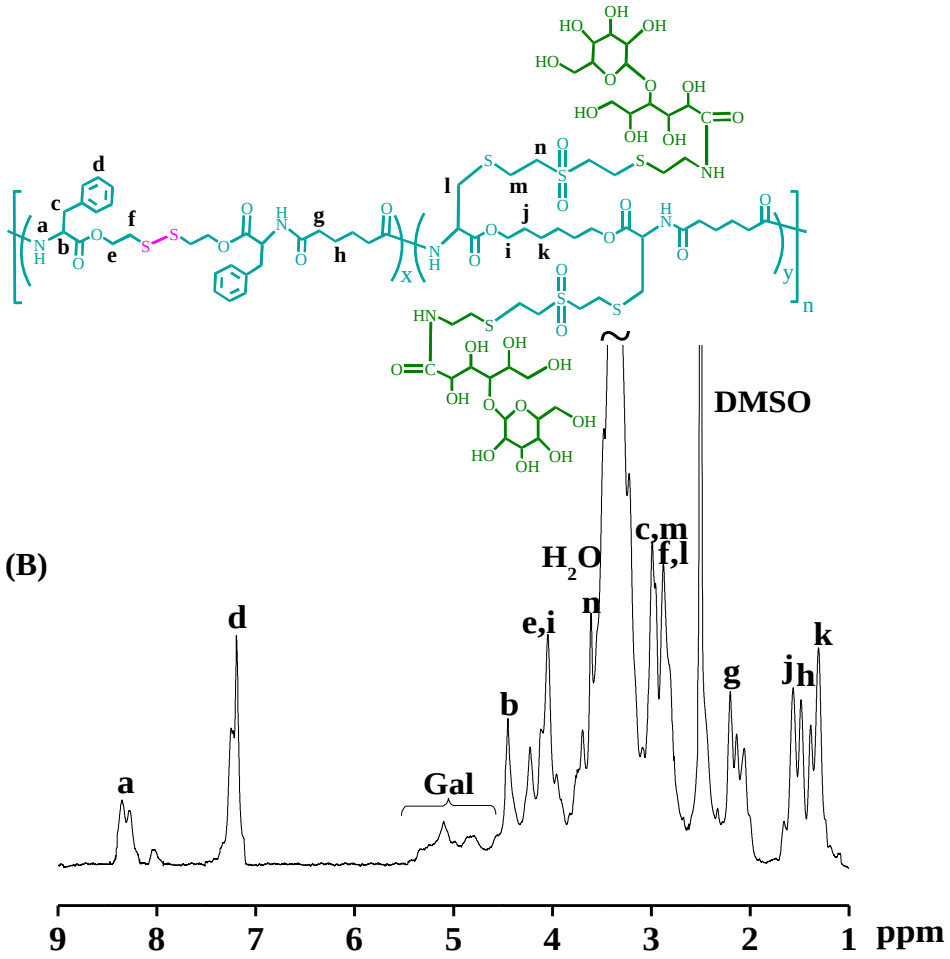

Fig. 1 ^{1}**H NMR spectra (400 MHz, DMSO-d_6) of SSPEA (A) and SSPEA-Gal (B).**

The post-polymerization modification of SSPEA with Gal-SH was carried out in DMSO at r.t. for 24 h, which readily yielded SSPEA-Gal graft copolymers. ^{1}H NMR showed that new peaks assignable to galactose moieties appeared at δ 3.6-3.8 and 4.7-5.4, while signals attributable to vinyl protons at δ 6.36-6.95 completely disappeared, corroborating quantitative coupling of Gal-SH (Fig. 1B). By using SSPEAs with different VSC contents in Table 1, SSPEA-Gal copolymers with different Gal contents of 31.6 wt.% and 42.5 wt.% were obtained accordingly (Table 2).

Using the same method, reduction-insensitive PEA-Gal was synthesized based on PEA with a [Phe(HD)]/[VSC(HD)] molar ratio of 4.8/5.2, M_n (^{1}H NMR) of 6.8 kg/mol, and a moderate PDI of 1.53 (Table 1, Entry 3).

Preparation of SSPEA-Gal Nanoparticles, Drug Loading, and In Vitro Drug Release

Micellar nanoparticles were readily prepared by solvent exchange method. Similar as PCL-g-SS-Gal graft copolymers,[39] SSPEA-Gal copolymers are stabilized by the hydrophilic Gal shells. The dynamic light scattering (DLS) measurements showed that all SSPEA-Gal copolymers self-assembled into nano-sized micellar particles with a unimodal distribution (Fig. 2A). SSPEA-Gal nanoparticles have average sizes decreased from ca. 138 to 91 nm with Gal contents increasing from 31.6 wt.% to 42.5 wt.% (Table 2). The increase in Gal content would lead to increase of steric repulsion and decrease of hydrophobic interactions, which favors formation of micellar nanoparticles with decreased micelle aggregation numbers and hence smaller particle sizes. The nanoparticles were denoted as SSPEA-GalX, wherein X represents Gal contents in weight percentage. TEM micrograph displayed that SSPEA-Gal42 nanoparticles had an average size of ca. 65 nm (Fig. 2B), which was somewhat smaller than that determined by DLS likely due to shrinkage of nanoparticles upon drying. The critical aggregation concentrations (CAC) were 3.47 and 8.56 mg/L for SSPEA-Gal42 and SSPEA-Gal32, respectively. As comparison, PEA-Gal42 nanoparticles were 97 nm in diameter and CAC of 2.58 mg/L (Table 2).

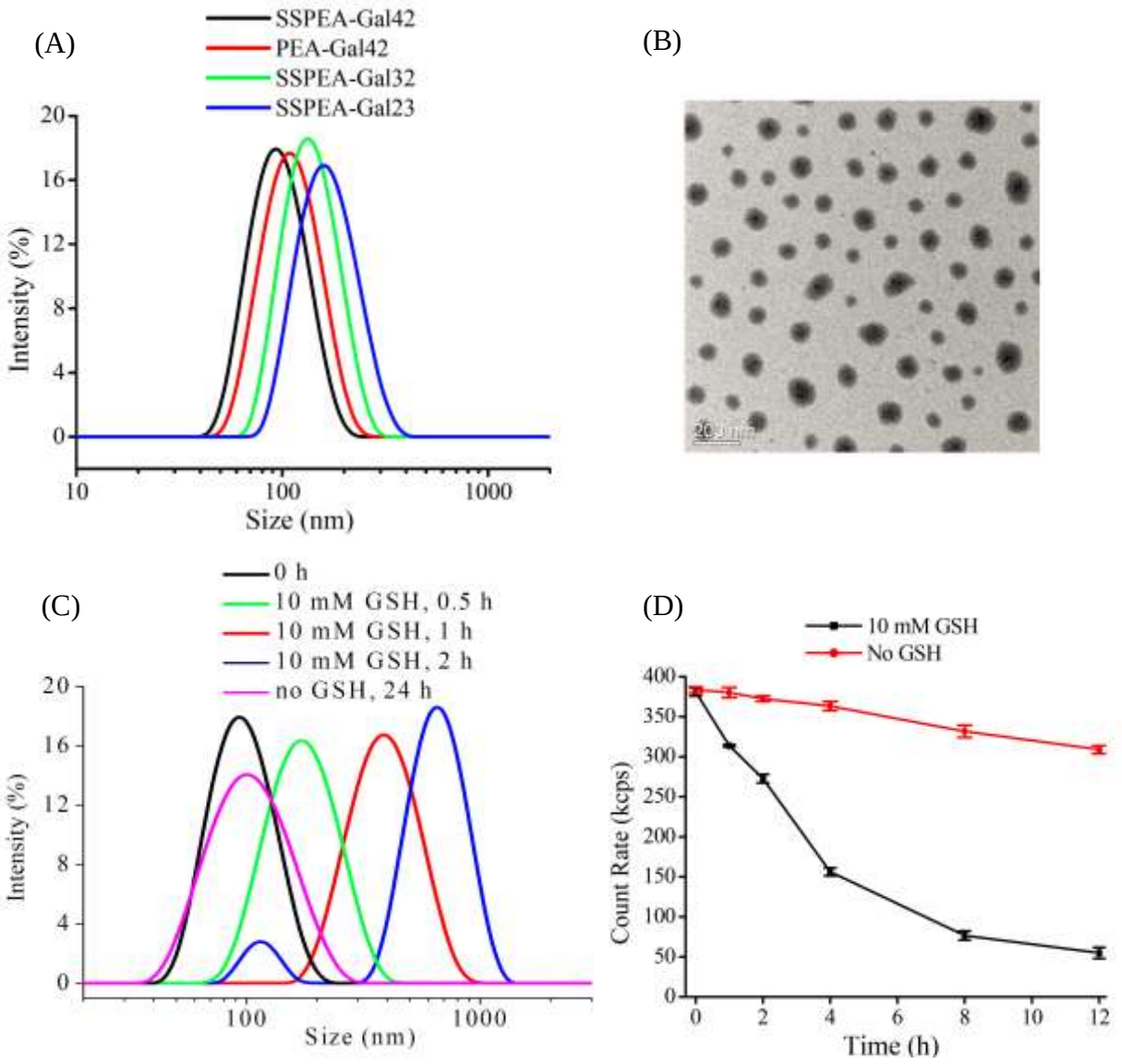

Fig. 2 DLS and TEM measurements of SS-PEA-Gal and PEA-Gal nanoparticles. (A) Size distribution profiles of SSPEA-Gal and PEA-Gal nanoparticles determined by DLS; (B) TEM micrograph of SSPEA-Gal42 nanoparticles; (C) Size change of SSPEA-Gal42 nanoparticles in response to 10 mM GSH in PBS (10 mM, pH 7.4) measured by DLS; and (D) The change of count rate of SSPEA-Gal42 at a concentration of 0.5 mg/mL in PBS (10 mM, 150 mM NaCl) containing 10% serum at pH 7.4 and 37 °C with or without 10 mM GSH monitored by DLS .

To investigate their reduction-sensitivity, size change of SSPEA-Gal nanoparticles in PBS at pH 7.4 in response to 10 mM GSH was monitored over time. The results showed that the size of SSPEA-Gal42 nanoparticles increased from 91 nm to 190 nm in 0.5 h, reaching over 600 nm after 2 h (Fig. 2C). In contrast, little size change was observed for SSPEA-Gal42

nanoparticles in 24 h under a non-reductive condition as well as for reduction-insensitive PEA-Gal42 nanoparticles in the presence of 10 mM GSH in 24 h (Fig. S5). It should further be noted that SSPEA-Gal42 nanoparticles were rather stable in 10% serum containing PBS at 37 °C, as revealed by little change in the count rate (scattering intensity) in 12 h (Fig. 2D). In contrast, the count rate dropped significantly in the presence of 10 mM GSH under otherwise the same conditions, in agreement with reduction-triggered shedding of Gal shells and destabilization of nanoparticles.

Table 2 Characteristics of SSPEA-Gal and PEA-Gal micellar nanoparticles.

Entry	Nanoparticles	Gal Content (*wt.*%)	Size (nm)[a]	PDI[a]	CAC (mg/L)[b]
1	SSPEA-Gal32	31.6	138 ± 3	0.12	8.56
2	SSPEA-Gal42	42.5	91 ± 3	0.10	3.47
3	PEA-Gal42	42.4	97 ± 2	0.09	2.58

[a] Determined by DLS.

[b] Determined by fluorescence measurement.

SSPEA-Gal nanoparticles showed decent DOX loading capacity with drug loading contents (DLC) of 4.1, 7.3 and 11.9 wt.%, which corresponded to drug loading efficiencies (DLE) of 86.4%, 78.7% and 67.5%, at theoretical DLC of 4.8, 9.1 and 16.7 *wt.*%, respectively, for SSPEA-Gal42 nanoparticles (Table 3). The size increased from ca. 105 to 143 nm with increasing drug loading levels. The size distributions, however, remained low (PDI = 0.12 – 0.16). PEA-Gal42 nanoparticles exhibited similar DOX loading and particle sizes.

The *in vitro* drug release studies showed that under an intracellular-mimicking reductive condition (in PBS at pH 7.4 and 37 ºC in the presence of 10 mM GSH), DOX was rapidly discharged from SSPEA-Gal42 nanoparticles, in which ca. 50 % and 80 % DOX was released in 2 and 12 h, respectively (Fig. 3). In contrast, less than 20 % drug release was observed in

12 h for reduction-insensitive PEA-Gal42 nanoparticles under otherwise the same conditions and for SSPEA-Gal42 nanoparticles under a non-reductive condition.

Table 3 DOX loading content and loading efficiency of nanoparticles.

Nanoparticles	DLC (*wt.*%)		DLE	Size	PDI [b]
	Theory	Determined[a]	(%)	(nm)[b]	
SSPEA-Gal42	4.8	4.1	86.4	105 ± 2	0.12
	9.1	7.3	78.7	122 ± 3	0.13
	16.7	11.9	67.5	143 ± 3	0.16
PEA-Gal42	4.8	4.0	84.2	112 ± 4	0.11
	9.1	7.5	81.5	133 ± 5	0.15
	16.7	12.4	70.5	154 ± 3	0.18

[a] Determined by fluorescence measurement.

[b] Size and PDI of DOX-loaded nanoparticles were determined by DLS.

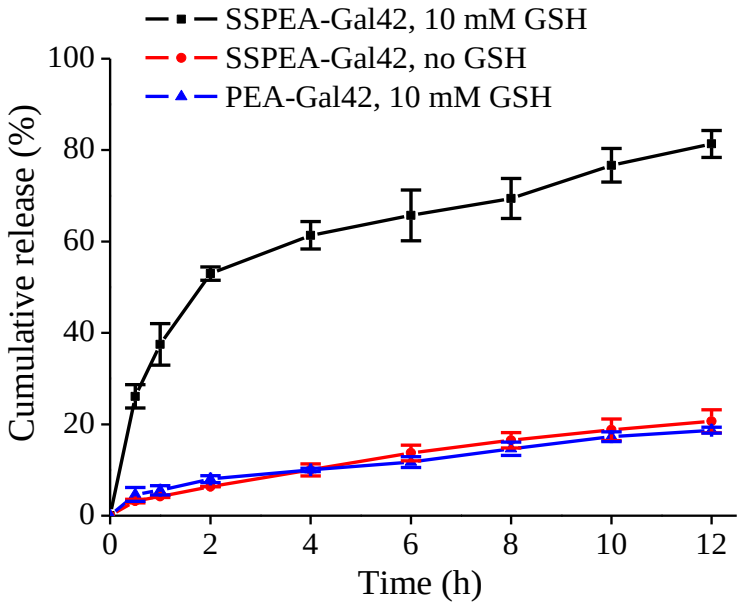

Fig. 3 The *in vitro* DOX release from SSPEA-Gal42 nanoparticles in PBS (pH 7.4, 10 mM, 150 mM NaCl) in the presence or absence of 10 mM GSH at 37 °C. DOX release from PEA-Gal42 nanoparticles in the presence of 10 mM GSH was used as control (n = 3). The initial micelle concentration was fixed at 0.2 mg/mL.

Targeted Antitumor Activity of DOX-Loaded SSPEA-Gal Nanoparticles

The anti-tumor activity of DOX-loaded SSPEA-Gal was investigated using MTT assays in ASGP-R over-expressing HepG2 cells. MCF-7 cells with low ASGP expression were used as a negative control. The results demonstrated that DOX-loaded SSPEA-Gal42 exhibited a high anti-tumor effect to HepG2 cells following 48 h incubation with a half maximal inhibitory concentration (IC_{50}) of 1.37 μg DOX equiv./mL, which was over 6 times lower than that of DOX-loaded reduction-insensitive PEA-Gal42 counterparts (Fig. 4A). Given the fact that SSPEA-Gal42 and PEA-Gal42 nanoparticles have similar surface properties, the lower IC_{50} is most probably due to the fast intracellular drug release from DOX-loaded SSPEA-Gal42 triggered by cytoplasmic GSH. In accordance, DOX-loaded SSPEA-Gal42 also displayed much higher anti-tumor activity than DOX-loaded PEA-Gal42 toward MCF-7 cells (Fig. 4B). It is noted that DOX-loaded SSPEA-Gal42 showed obviously higher cytotoxicity to HepG2 cells than to MCF-7 cells (IC_{50} 1.37 *vs.* 3.64 μg DOX equiv./mL), supporting specific recognition and efficient cellular uptake of SSPEA-Gal42 by the ASGP receptor overexpressing HepG2 cells. Moreover, DOX-loaded SSPEA-Gal42 exhibited much higher antitumor effect in HepG2 cells as compared to DOX-loaded SSPEA-Gal32 (IC_{50} 1.37 *vs.* 4.99 μg DOX equiv./mL) (Fig. 4), signifying that Gal density plays an important role in the targetability and cytotoxicity of DOX-loaded SSPEA-Gal nanoparticles to HepG2 cells.

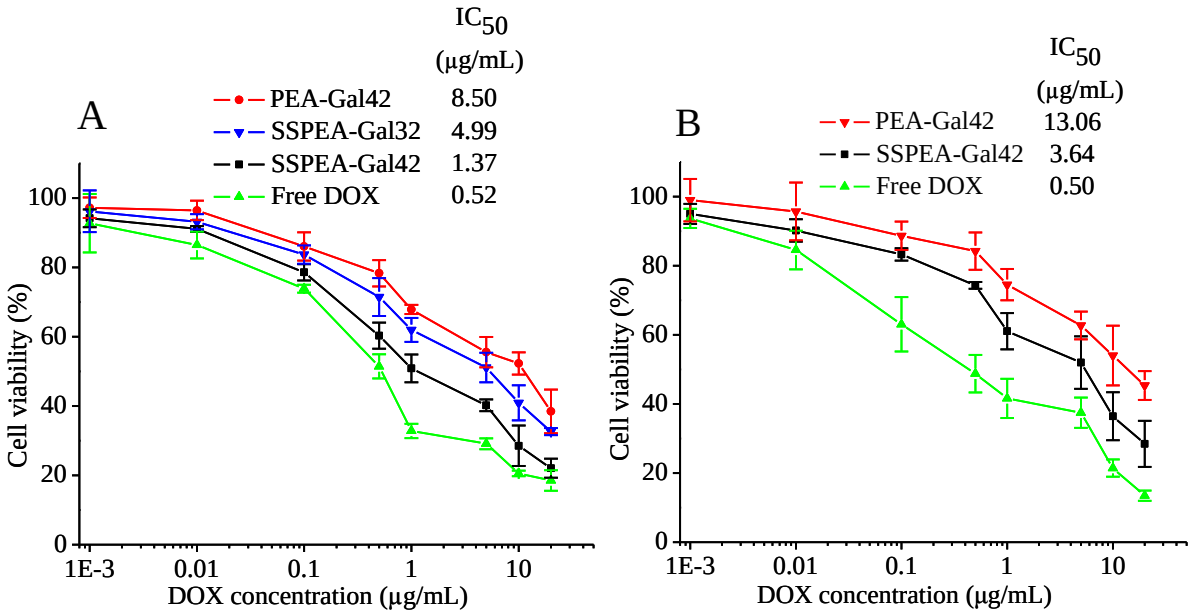

Fig. 4 The antitumor activity of DOX-loaded SSPEA-Gal42 and PEA-Gal42 to HepG2 cells (A) and MCF-7 cells (B). Free DOX was used as a control. The cells were incubated with DOX-loaded nanoparticles or free DOX for 48 h at DOX concentrations ranging from 1.0×10^{-3} to 20 μg/mL. Data are presented as the average ± SD (n = 4).

The targetability of DOX-loaded SSPEA-Gal42 to HepG2 cells was further confirmed by competitive inhibition experiments. The results revealed that pretreating HepG2 cells with free LBA, thereby blocking ASGP-R receptors, led to significant increase of cell viability from ca. 59 % to 89 % (Fig. 5A). In contrast, the LBA pretreatment had little influence on the cytotoxicity of SSPEA-Gal42 to MCF-7 cells (Fig. 5B). These results point out that SSPEA-Gal possesses excellent targetability to HepG2 cells and can efficiently deliver and release DOX into target cells inducing effective cell death. It is noteworthy to note that both SSPEA-Gal42 and PEA-Gal42 were practically nontoxic to HepG2 and MCF-7 cells (cell viabilities > 92%) up to a tested concentration of 1.0 mg/mL (Fig.S6). The potential degradation product, mercaptoethanol, following complete degradation of SSPEA-Gal42 polymer might cause toxic effect. The observed low cytotoxicity of SSPEA-Gal42 nanoparticles is possibly due to the fact that polymers were degraded into mercaptoethanol derivatives and there was little mercaptoethanol if present.

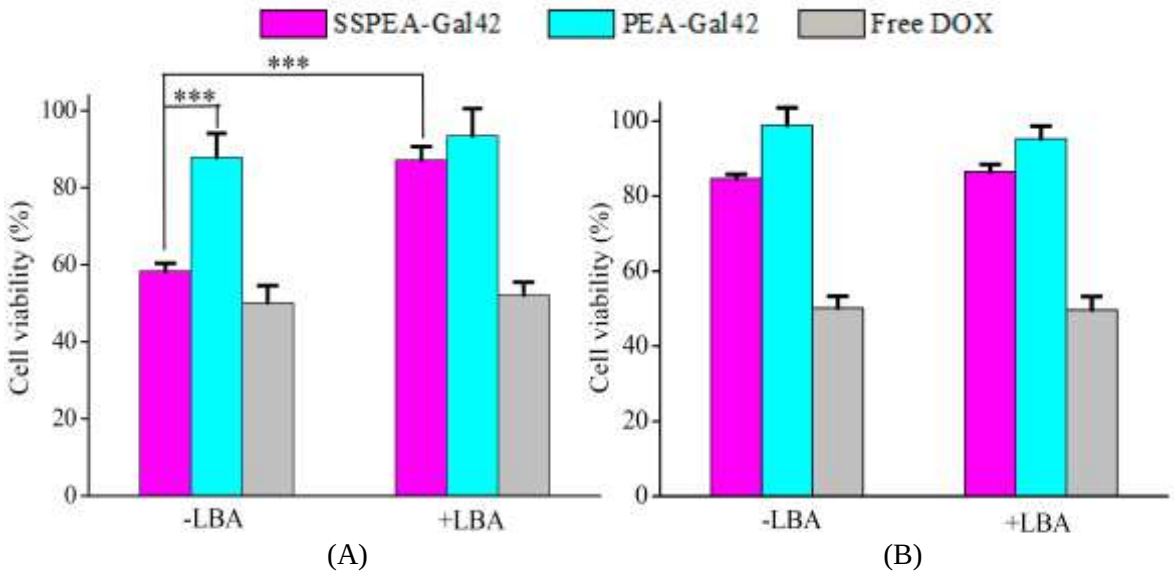

Fig. 5 Cytotoxicity of DOX-loaded SSPEA-Gal42, PEA-Gal42 nanoparticles and free DOX to HepG2 cells (A) and MCF-7 cells (B) (DOX dosage: 10 μg/mL). The cells were either pretreated with LBA (+LBA) for 4 h or without pretreatment (-LBA). The cells were incubated with DOX-loaded nanoparticles or free DOX for 4 h, the medium was replaced with fresh medium, and the cells were further cultured for 44 h. Data are presented as the average ± SD (n = 4, Student's *t* test, ***p < 0.001).

Cellular Uptake and Intracellular Drug Release

The cellular uptake and intracellular release of DOX from SSPEA-Gal42 nanoparticles were evaluated using flow cytometry and CLSM. The flow cytometry results showed that cellular DOX level in HepG2 cells treated with DOX-loaded SSPEA-Gal42 was ca. 3-fold higher than that with DOX-loaded PEA-Gal42 (reduction-insensitive control) (Fig. 6). Previous studies have shown that fluorescence of DOX inside nanoparticles is largely self-quenched.[46] The higher cellular DOX level observed for DOX-loaded SSPEA-Gal42 is most likely related to its fast DOX release inside HepG2 cells. The competitive inhibition experiments showed that pretreatment of HepG2 cells with free LBA resulted in obviously decreased cellular DOX level (Fig. 6), supporting that DOX-loaded SSPEA-Gal42 is internalized by HepG2 cells via a

receptor-mediated mechanism.

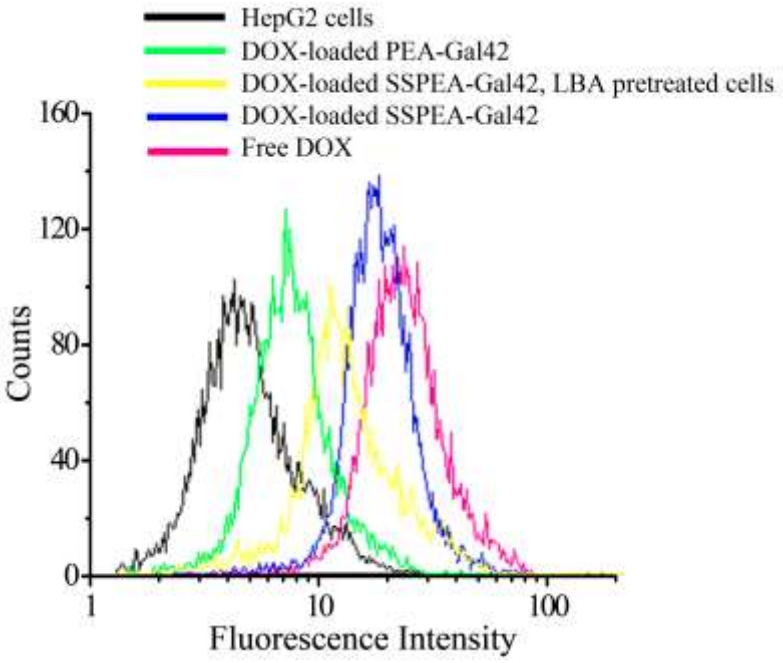

Fig. 6 Flow cytometric analysis on the cellular internalization of DOX-loaded SSPEA-Gal42 and DOX-loaded PEA-Gal42 into HepG2 cells and LBA pretreated HepG2 cells (+LBA) following 24 h incubation (DOX dosage: 10 μg DOX equiv./mL, micelle concentration: 0.2 mg/mL, cell counts of 10000). HepG2 cells and free DOX were used as controls.

CLSM studies demonstrated that strong DOX fluorescence was observed in HepG2 cells following 4 h incubation with DOX-loaded SSPEA-Gal42, and a significant amount of DOX entered the nuclei (Fig. 7A), which was similar to HepG2 cells treated with free DOX (Fig. 7D), in accordance with efficient cellular uptake and intracellular drug release. In comparison, less DOX fluorescence and little in the nuclei was detected in MCF-7 cells following 4 h treatment with DOX-loaded SSPEA-Gal42 under otherwise the same conditions (Fig. 7B). Moreover, weak DOX fluorescence was observed in HepG2 cells treated with DOX-loaded PEA-Gal42 (Fig. 7C), confirming significant role of reductive degradation in intracellular DOX release. These results corroborate that SSPEA-Gal42 have high targetability to HepG2 cells and efficient intracellular drug release. The superior specificity and antitumor efficacy toward hepatocellular carcinoma cells, low cytotoxicity, and facile preparation renders

SSPEA-Gal nanoparticles interesting for targeted chemotherapy of hepatocellular carcinoma *in vivo*.

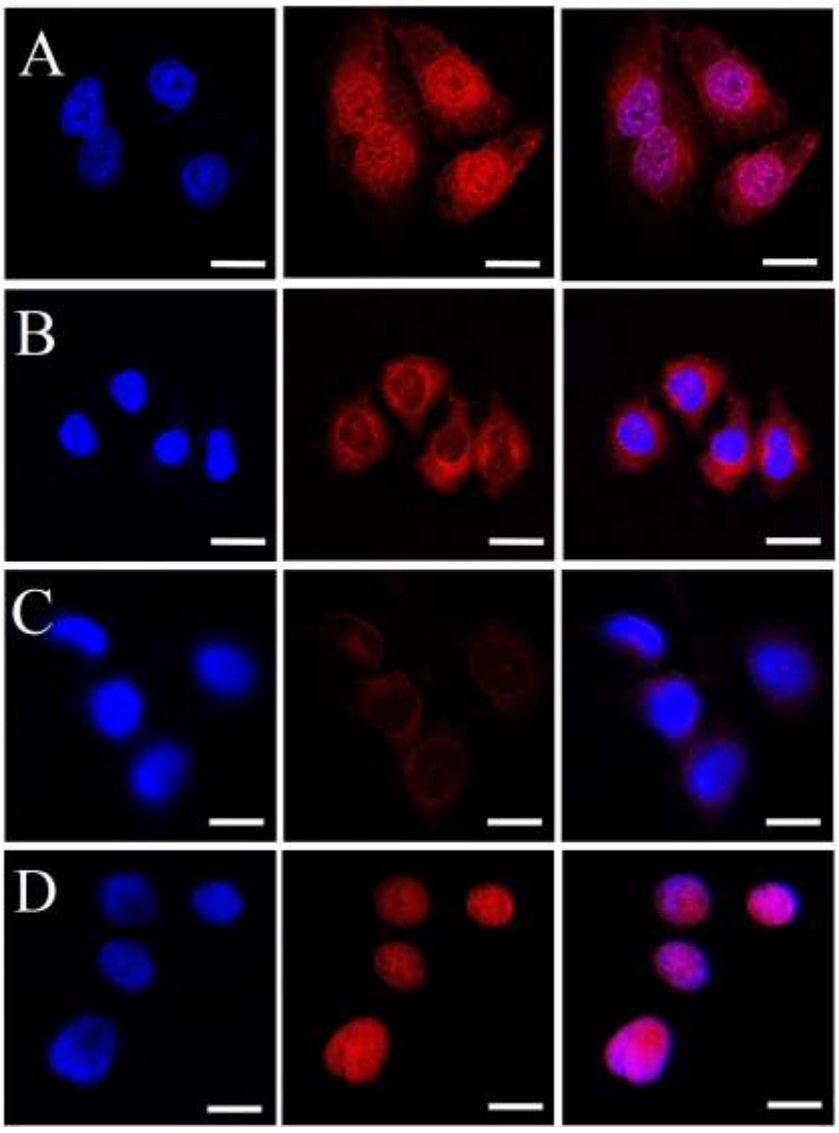

Fig. 7 CLSM images of HepG2 cells treated with DOX-loaded SSPEA-Gal42 (A), MCF-7 cells treated with DOX-loaded SSPEA-Gal42 (B), HepG2 cells treated with DOX-loaded PEA-Gal42 (C), and HepG2 cells treated with free DOX (D). The cells were incubated with drug-loaded nanoparticles or free DOX for 4 h (DOX dosage: 10 μg DOX equiv./mL). For each panel, the images from left to right were cell nuclei stained by DAPI (blue), DOX fluorescence (red), and overlays of the above two images. The scale bars represents 20 μm.

Conclusions

We have demonstrated that galactose-decorated reduction-sensitive degradable nanoparticles

prepared from α-amino acid-based poly(ester amide)-graft-galactose graft copolymers (SSPEA-Gal) present superior specificity and antitumor activity to HepG2 cells. These smart yet simple nano-vehicles offer several attractive features: (i) α-amino acid-based SSPEA-Gal are biodegradable and nontoxic, and could be readily prepared with tunable galactose densities; (ii) SSPEA-Gal form small-sized micellar nanoparticles with decent drug loading capacity, in which galactose acts hydrophilic shell and reduction-sensitive enzymatically degradable poly(ester amide) as a hydrophobic core; and (iii) DOX-loaded nanoparticles show apparent targetability to hepatoma cells as well as fast intracellular DOX release, resulting in high specificity and antitumor effect to hepatocellular carcinoma cells *in vitro*. This study presents a novel and versatile strategy to fabricate tumor-targeting nanoparticles, *i.e.* grafting a hydrophilic targeting ligand onto a stimuli-sensitive degradable polymer backbone. In the following, we will study the *in vivo* targeting and therapeutic performance of DOX-loaded nanoparticles in the treatment of human hepatoma xenografts in nude mice.

Acknowledgements

This work is financially supported by research grants from the National Natural Science Foundation of China (NSFC 51103093, 51173126 and 51473111), the National Science Fund for Distinguished Young Scholars (NSFC 51225302), the major project of Jiangsu province university natural science (14KJA150008), Ph.D. Programs Foundation of Ministry of Education of China (20133201110005), and a Project Funded by the Priority Academic Program Development (PAPD) of Jiangsu Higher Education Institutions.

References

1 H. Tian, Z. Tang, X. Zhuang, X. Chen and X. Jing, *Prog. Polym. Sci.*, 2012, **37**, 237.

2 H. Seyednejad, A. H. Ghassemi, C. F. van Nostrum, T. Vermonden and W. E. Hennink, *J. Control. Release*, 2011, **152**, 168.

3 J. Feng, R.-X. Zhuo and X.-Z. Zhang, *Prog. Polym. Sci.*, 2012, **37**, 211.

4 C. Deng, J. T. Wu, R. Cheng, F. H. Meng, H.-A. Klok and Z. Y. Zhong, *Prog. Polym. Sci.*, 2014, **39**, 330.

5 B. Tian, X. Tao, T. Ren, Y. Weng, X. Lin, Y. Zhang and X. Tang, *J. Mater. Chem.*, 2012, **22**, 17404.

6 J. Huang and A. Heise, *Chem. Soc. Rev.*, 2013, **42**, 7373.

7 A. C. Fonseca, M. H. Gil and P. N. Simões, *Prog. Polym. Sci.*, 2014, **39**, 1291.

8 A. Rodriguez-Galan, L. Franco and J. Puiggali, *Polymers*, 2011, **3**, 65.

9 H. L. Sun, F. H. Meng, A. A. Dias, M. Hendriks, J. Feijen and Z. Y. Zhong, *Biomacromolecules*, 2011, **12**, 1937.

10 Y. Feng, J. Lu, M. Behl and A. Lendlein, *Macromol. Biosci.*, 2010, **10**, 1008.

11 D. K. Knight, E. R. Gillies and K. Mequanint, *Acta Biomater.*, 2014, **10**, 3484.

12 J. Wu, D. Yamanouchi, B. Liu and C.-C. Chu, *J. Mater. Chem.*, 2012, **22**, 18983.

13 J. Wu and C.-C. Chu, *J. Mater. Chem. B*, 2013, **1**, 353.

14 J. Wu, X. Zhao, D. Wu and C.-C. Chu, *J. Mater. Chem. B*, 2014, **2**, 6660.

15 M. X. Deng, J. Wu, C. A. Reinhart-King and C.-C. Chu, *Biomacromolecules*, 2009, **10**, 3037.

16 M. X. Deng, J. Wu, C. A. Reinhart-King and C.-C. Chu, *Acta Biomater.*, 2010, **7**, 1504.

17 K. Guo and C. C. Chu, *J. Appl. Polym. Sci.*, 2010, **117**, 3386.

18 X. Pang and C.-C. Chu, *Biomaterials*, 2010, **31**, 3745.

19 H. T. Cui, Y. D. Liu, M. X. Deng, X. Pang, P. B. Zhang, X. H. Wang, X. S. Chen and Y. Wei, *Biomacromolecules*, 2012, **13**, 2881.

20 A. Ghaffar, G. J. J. Draaisma, G. Mihov, A. A. Dias, P. J. Schoenmakers and S. van der Wal, *Biomacromolecules*, 2011, **12**, 3243.

21 M. Y. He, A. Potuck, Y. Zhang and C.-C. Chu, *Acta Biomater.*, 2014, **10**, 2482.

22 X. Pang and C.-C. Chu, *Polymer*, 2010, **51**, 4200.

23 J. S. Mejia and E. R. Gillies, *Polym. Chem.*, 2013, **4**, 1969.

24 P. J. Sun, D. h. Zhou and Z. H. Gan, *J. Control. Release*, 2011, **155**, 96.

25 H. L. Sun, F. H. Meng, R. Cheng, C. Deng and Z. Y. Zhong, *Exp. Opin. Drug Deliv.*, 2013, **10**, 1109.

26 B. Khorsand, G. Lapointe, C. Brett and J. K. Oh, *Biomacromolecules*, 2013, **14**, 2103.

27 W. Chen, M. Zheng, F. H. Meng, R. Cheng, C. Deng, J. Feijen and Z. Y. Zhong, *Biomacromolecules*, 2013, **14**, 1214.

28 X. J. Cai, C. Y. Dong, H. Q. Dong, G. M. Wang, G. M. Pauletti, X. J. Pan, H. Y. Wen, I. Mehl, Y. Y. Li and D. L. Shi, *Biomacromolecules*, 2012, **13**, 1024.

29 R. Cheng, F. Feng, F. H. Meng, C. Deng, J. Feijen and Z. Y. Zhong, *J. Control. Release*, 2011, **152**, 2.

30 F. H. Meng, W. E. Hennink and Z. Y. Zhong, *Biomaterials*, 2009, **30**, 2180.

31 J. Chen, F. Zehtabi, J. Ouyang, J. M. Kong, W. Zhong and M. M. Xing, *J. Mater. Chem.*, 2012, **22**, 7121.

32 C. Cui, Y.-N. Xue, M. Wu, Y. Zhang, P. Yu, L. Liu, R.-X. Zhuo and S.-W. Huang, *Biomaterials*, 2013, **34**, 3858.

33 Y.-C. Wang, F. Wang, T.-M. Sun and J. Wang, *Bioconjugate Chem.*, 2011, **22**, 1939.

34 J. Yang, W. Liu, M. Sui, J. Tang and Y. Shen, *Biomaterials*, 2011, **32**, 9136.

35 J. Li, M. R. Huo, J. Wang, J. P. Zhou, J. M. Mohammad, Y. L. Zhang, Q. N. Zhu, A. Y. Waddad and Q. Zhang, *Biomaterials*, 2012, **33**, 2310.

36 Z. Y. Xiao and O. C. Farokhzad, *ACS Nano*, 2012, **6**, 3670.

37 J. Yue, S. Liu, R. Wang, X. L. Hu, Z. G. Xie, Y. B. Huang and X. B. Jing, *Mol. Pharm.*, 2012, **9**, 1919.

38 Y. N. Zhong, W. J. Yang, H. L. Sun, R. Cheng, F. H. Meng, C. Deng and Z. Y. Zhong, *Biomacromolecules*, 2013, **14**, 3723.

39 W. Chen, Y. Zou, F. H. Meng, R. Cheng, C. Deng, J. Feijen and Z. Y. Zhong, *Biomacromolecules*, 2014, **15**, 900.

40 Y. Li, Z.-Y. Tang and J.-X. Hou, *Nat. Rev. Gastroenterol. Hepatol.*, 2011, **9**, 32.

41 P. A. Ma, S. Liu, Y. B. Huang, X. S. Chen, L. P. Zhang and X. B. Jing, *Biomaterials*, 2010, **31**, 2646.

42 L. W. Seymour, D. R. Ferry, D. Anderson, S. Hesslewood, P. J. Julyan, R. Poyner, J. Doran, A. M. Young, S. Burtles and D. J. Kerr, *J. Clin. Oncol*, 2002, **20**, 1668.

43 R. Yang, F. H. Meng, S. B. Ma, F. S. Huang, H. Y. Liu and Z. Y. Zhong, *Biomacromolecules*, 2011, **12**, 3047.

44 Y. Zou, Y. Song, W. J. Yang, F. H. Meng, H. Y. Liu and Z. Y. Zhong, *J. Control. Release*, 2014, **193**, 154.

45 K. Guo and C. C. Chu, *Biomacromolecules*, 2007, **8**, 2851.

46 H. L. Sun, B. N. Guo, R. Cheng, F. H. Meng, H. Y. Liu and Z. Y. Zhong, *Biomaterials*, 2009, **30**, 6358.